SUPPLEMENTARY INFORMATION

USP25 promotes pathological HIF-1-driven metabolic reprogramming and is a potential therapeutic target in pancreatic cancer

Jessica K. Nelson, May Zaw Thin, Theodore Evan, Steven Howell, Mary Wu, Bruna Almeida, Nathalie Legrave, Duco S. Koenis, Gabriela Koifman, Yoichiro Sugimoto, Miriam Llorian Sopena, James MacRae, Emma Nye, Michael Howell, Ambrosius P. Snijders, Andreas Prachalias, Yoh Zen, Debashis Sarker, and Axel Behrens

Supplementary Figure 1 (related to Figure 1). Characterization of enzymatically active DUBs in PDAC using activity-based proteomics. (a) In-gel visualization of Cy5-Ub-ABP labelled DUBs in KPCY-organoids. (b) Mass spectrometry analysis of DUBs labelled with Biotin-ubiquitin-ABP in KPCY organoids. Volcano blot depicts the label-free quantification (LFQ) of -$\log_{10}$ t-test p-value vs ratio difference of untreated (right side) and DUBi-treated (left side) samples. (c) Volcano plot shows the significance of each gene set from the Gene Ontology (GO) biological Process 2021 dataset versus its odds ratio from mass spectrometry data in Figure 1c. Each point represents a single geneset; the x-axis measures the odds ratio (0, inf) calculated for the gene set, while the y-axis gives the -log(p-value) of the gene set. Larger blue points represent significant terms (p-value < 0.05); smaller grey points represent non-significant terms. The darker the blue colour of a point, the more significant it is. (d) Bar chart shows the top 10 enriched terms in the GO Biological Process 2021 library, along with their corresponding p-values. (e) Mass spectrometry analysis of DUBs labelled with Biotin-ubiquitin-ABP in KPCY tumor tissue, with or without DUBi treatment (n=3 biologically independent samples per group). Displayed as median normalized -$\log_{10}$ t-test p-value vs ratio difference of untreated (right side) and DUBi-treated (left side) samples. For (b and e) grey dots indicate all proteins identified, and red dots highlight all significant DUBs. Source data are provided as a Source Date file.

Supplementary Figure 2 (related to Figure 2). Genetic knock-down screen identifies Usp25 as an essential DUB in PDAC organoids. (a) Representative images of KPCY organoids following puromycin selection with non-targeting (NT) or YFP-targeting shRNAs. Scale bar is 800 μM. (b) Quantification of YFP signal from (a), shown as mean fluorescent intensity (MFI), and displayed as mean ± SD. Statistical

significance was determined by two-sided Student's t-test (n=6 biologically independent experiments). (c) Quantification of organoid growth calculated by % well confluency from live-cell phenotypic monitoring system, and displayed as mean ± SD. Statistical significance was determined by two-sided Student's t-test (n=6 biologically independent experiments). (d) Organoid viability was measured after 72 hours post puromycin selection and shown as relative luminescent unit (RLU), and displayed as mean ± SD. Statistical significance was determined by two-sided Student's t-test (n=6 biologically independent experiments). (e) Representative images from live-cell phenotypic monitoring time-course in KPCY organoids. Confluency mask is shown in yellow. Scale bar is 1 mm. (f) Quantitative values are plotted from two representative control shRNA lines are shown, with a peak growth confluency between 72-90 hours, highlighted with red dashed bars in (f), and red box in (e). Black dashed lines highlight 24- and 114-hour images in (e). Source data are provided as a Source Date file.

Supplementary Figure 3 (related to Figure 3). USP25 is highly expressed and enzymatically active in PDAC compared to normal pancreatic tissue, which correlated with poor patient survival. (a) Histological and immunohistochemical analysis of Usp25 expression in normal pancreatic and KPCY tumor tissues. Scale bar is 100 μm. Each image comes for a biologically independent animal, quantified in Figure 3b (b) Histological and immunohistochemical analysis of USP25 staining in primary patient PDAC tumors. Scale bar is 1000 μm and insert is 100 μm. Each image comes from an independent patient.

Supplementary Figure 4 (related to Figure 4). Depletion of *USP25* leads to reduced patient-derived organoid formation, viability and attenuated PDAC

tumor growth *in vivo.* (a) Representative brightfield images of sh*Usp25* silencing in KPCY organoids. Scale bar is 800 µm. (b) Expression of *Usp25* in KPCY organoids and displayed as relative mRNA expression compared to shYFP controls. Data shown as mean ± SD, and statistical significance was determined by One-way ANOVA with Dunnett post-hoc test (n=4 biologically independent samples). (c) Expression of *USP25* in PDO lines and displayed as relative mRNA expression compared to shNT controls. Data shown as mean ± SD, and statistical significance was determined by One-way ANOVA with Dunnett post-hoc test (n=4 biologically independent samples). (d) Representative images of sh*USP25* silencing in PDOs incubated with caspase-3 activity probe. Scale bar is 800 µm. (e) Schematic of *USP25* knock-out strategy using CRISPR/Cas9. (f) Sanger sequencing data of the USP25 locus from PDO line (K17T) parental and *USP25* knock-out clones. (g) Representative images of the Hu-PDAC organoids, showing empty vector (EV) control and CRISPR/Cas9-mediated *USP25* knock-out cells. Each USP25$^{-/-}$ clones are described with single guide (sg) targeting exon shown. Scale bar is 400 µm. (h) Organoid viability displayed as % relative to the EV, and shown as mean ± SD. Statistical significance was determined by One-way ANOVA with Dunnett post-hoc test (n=3 biologically independent experiments). Source data are provided as a Source Date file.

Supplementary Figure 5 (related to Figure 5). Transcriptional and metabolomic profiling of PDAC organoids reveals USP25 as a novel regulator of HIF-1 transcriptional activity and metabolic rewiring. (a) Principal component analysis of log-transformed normalized counts for the top 5000 most variable transcripts (as determined by standard deviation) from the RNA-seq experiment. (b) Hierarchical clustering of log-transformed and mean-centered normalized counts for all

differentially expressed transcripts from the RNA-seq experiment. (c-d) Pathway analysis of differentially expressed genes down-regulated upon loss of *Usp25*. Bar chart shows the top 10 enriched terms in the (c) MsigDB Hallmark 2020 and (d) KEGG 2021 libraries, along with their corresponding p-values. (e-f) Spearman correlation of *USP25* gene expression with gene signatures from (e) the KEGG glycolysis pathway or (f) the HALLMARK hypoxia pathway. Data in (e-f) generated from the GEPIA database, where each dot represents data from one patient expressed as transcripts per million (TPM).

Supplementary Figure 6 (related to Figure 5). Transcriptional and metabolomic profiling of PDAC organoids reveals USP25 as a novel regulator of HIF-1 transcriptional activity and metabolic rewiring. (a) Heatmap of gene expression z-scores for the HALLMARK Hypoxia pathway (ID:M5891). (b) Gene expression in KPCY organoids, displayed as relative mRNA expression compared to shYFP controls. Data shown as mean ± SD, and statistical significance was determined by two-sided Students t-test with Holm-Sidak post-hoc correction for multiple testing (n=4 biologically independent experiments). (c) Glucose concentrations measured in culture medium from Mu KPCY organoids, and displayed as mean ± SD. Statistical significance was determined by two-sided Students t-test with Holm-Sidak post-hoc correction for multiple testing (n=3 biologically independent experiments). (d-e) Incorporation of ^{13}C-glucose into (d) intracellular pyruvate, and (e) TCA metabolites in treated KPCY organoids. Data in (d-e) is displayed as mean ± SD, and represents one experiment carried out with six replicates. Due to technical limitations, statistics for (d-e) were performed on technical replicates using two-sided Student's t-test. Source data are provided as a Source Date file.

Supplementary Figure 7 (related to Figure 6). USP25 interacts with, deubiquitylates and stabilizes HIF-1α and promotes its transcriptional activity. (a) Western blot of indicated targets following siRNA-mediated knock-down of *USP25* or non-targeting (NT) control in human PDAC cell lines, treated with 200 μM cobalt chloride ($CoCl_2$) for six hours. (b) PDOs (line K13T) were treated with the cell-permeable Image-IT Red Hypoxia reagent to measure cellular hypoxia. Scale bar is 100μm. (c) Organoid viability in indicated PDO lines measured at day 5 under high oxygen tension (20%) or low oxygen tension (1%) culture conditions. Values shown as relative luciferase unit (RLU), and displayed as mean ± SD. Statistical significant was determined by two-way ANOVA with post hoc corrections for multiple testing (n= 4 biologically independent experiments). (d) Western blot of indicated targets following shRNA-mediated knock-down of *USP25* or non-targeting control in PDOs (line K13T), with 200 μM $CoCl_2$ treatment for six hours where indicated. Source data are provided as a Source Date file.

Supplementary Figure 8 (related to Figure 6). USP25 interacts with, deubiquitylates and stabilizes HIF-1α and promotes its transcriptional activity. (a) HEK293T transfected with the indicated expression constructs for epitope-tagged USP25 and HIF-1α. GFP was co-transfected as a transfection efficiency and additional loading control. 24 hours post-transfection, cells were treated for an additional 24 hours with 200 μM $CoCl_2$. Total cell lysates were immunoblotted or immunoprecipitated and analyzed as indicated. (b) Human renal carcinoma cell line RCC-4 was treated for 72 hours with siRNA for non-targeting (siNT) or four individual *USP25* targeting siRNA (*siUSP25* 1-4). Total cell lysates were immunoblotted as

indicated. (c) Western blot of indicated targets following siRNA-mediated knock-down of *USP25* or non-targeting control. (d) HEK293T cells transfected with indicated expression constructs for epitope-tagged HIF-1α and USP25 and treated with 200 µM cobalt chloride ($CoCl_2$) for six hours. Sub-cellular fractionation was done to compare cytosolic and nuclear expression of indicated targets. (e) *SLC2A1* mRNA expression in HEK293T cells, displayed as relative mRNA expression compared to EV transfected control. Data shown as mean ± SD, and statistical significance was determined by One-way ANOVA with Dunnett post-hoc test (n=4 biologically independent experiments). (f) Schematic of the lentiviral pInducer20-blast construct which was used to engineer PDO lines with DOX-inducible USP25 wild-type (WT) or catalytic mutant (C178S) expression. (g) Western blot images of endogenous protein levels following 48 hours of 1 µM DOX treatment in PDOs (line K13T) with DOX-inducible USP25-WT or -C178S expression. (h) Gene expression in PDOs, displayed as relative mRNA expression compared to controls (grey bars). Each bar represents the mean ± SD, and each symbol represents a different shRNA targeting either *HIF1A* or YFP control from the average of three biologically independent PDO lines. Statistical significance was determined by two-sided Students t-test with Holm-Sidak post-hoc correction for multiple testing. (i) Western blot images of protein levels following 72 hours of 500 nM DOX to induce expression of the HA-tagged HIF-1α stabilization mutant ($HIF1A^{P402A/P456A}$) in indicated PDO lines. Source data are provided as a Source Date file.

Supplementary Figure 9 (related to Figure 7). Pharmacological inhibition of USP25 leads to loss of HIF-1α signaling and reduced tumor growth *in vitro* and *in vivo*. (a) Brightfield images of Mu wild-type (WT) and KPCY organoids treated with

100nM FT206. Scale bar is 500 µm. (b) Total cell lysates were immunoblotted as indicated. (c) *Usp28* knock-out organoids treated with FT206 at the indicated doses for 72 hours. Organoid viability was displayed as % relative to vehicle-treated control, and shown as mean ± SD. Statistical significance was determined by One-way ANOVA with Dunnett post-hoc test (n=3 biologically independent experiments). (d) Representative brightfield images from (Figure 7c) of PDO lines treated with vehicle or 100nM FT206. Scale bar is 0.5 mm. (e) Gene expression in KPCY organoids, displayed as relative mRNA expression compared to vehicle-treated controls. Data shown as mean ± SD, and statistical significance was determined by two-sided Student's t-test with Holm-Sidak post-hoc correction for multiple testing (n=4 biologically independent experiments). (f) Heatmap displaying organoid viability in KPCY organoids treated with FT206 or different tankyrase and Wnt signaling inhibitors at indicated concentrations, displayed as relative luciferase unit (RLU). (g) Heatmap displaying organoid viability of PDO lines treated AZ6102 with indicated concentrations, calculated as % of vehicle-treated. Source data are provided as a Source Date file.

Supplementary Figure 10 (related to Figure 7). Pharmacological inhibition of USP25 leads to loss of HIF-1α signaling and reduced tumor growth *in vitro* and *in vivo*. (a) Subcutaneous tumor weights at endpoint from experiments derived with different KPCY organoid lines. Data displayed as mean ± SD, and statistical significance was determined by two-sided Student's t-test (KPCY-1 is equal to n=6 biologically individual animals per group, and KPCY-2 and -3 are equal to n=5 biologically individual animals per group). (b) Body weights of animals treated with FT206 (75 mg/kg) or vehicle, three times a week for 5 weeks. Data plotted as mean ±

SD (n=5 biologically individual animals per group). (c) Growth curves of PDOX volumes (line K3T), treated with vehicle or FT206. Data plotted as mean ± SD, and statistical significance was determined by Two-way ANOVA (n=5 biologically individual animals per group). (d) Representative images of 3D ultrasound images of PDOXs described in (c). Scale bar is 3mm (e) Endpoint tumor volumes (mm^3) of PDOX, from lines K3T (n=5 biologically individual animals per group) and K10T (n=6 biologically individual animals per group). Statistical significance was determined by two-sided Student's t-test. (f) Body weights of animals treated with FT206 (75 mg/kg) or vehicle, two-three times a week for 6 weeks. Data plotted as mean ± SD (n=5 biologically individual animals per group). (g) Representative immunohistochemical analysis of active cleaved caspase-3 (C3A) expression in subcutaneous KPCY organoid tumors. Scale bar is 1000 μm. Quantification shown in Figure 7h. Source data are provided as a Source Date file.

Supplementary Figure 11 (related to Figure 7). Pharmacological inhibition of USP25 leads to loss of HIF-1α signaling and reduced tumor growth *in vitro* and *in vivo*. (a) Representative images of immunofluorescent staining of DAPI (grey), CK19 (blue) and hypoxyprobe (red) in PDOX treated with vehicle or FT206. Scale bar is 1000 μm, and insert is 100 μm. (b) Quantification of hypoxyprobe positive staining area in whole tumor sections. Data displayed as mean ± SD, and statistical significance was determined by two-sided Student's t-test (n=14 biologically independent animals for vehicle and n=10 biologically independent animals for FT206 groups). (c) Representative images of immunofluorescent staining of Slc2a1 (red) and Lectin (blue) in KPCY subcutaneous tumors treated with vehicle or FT206. Scale bar is 1000 μm, and insert b and d are 100 μm. (d) Quantification of Slc2a1 positive

staining area, displayed as mean ± SD. Statistical significance was determined by two-sided Student's t-test (n=8 biologically independent animals per group). (e) Quantification of Lectin positive staining area, displayed as mean ± SD. Statistical significance was determined by two-sided Student's t-test (n=8 biologically independent animals per group). (f) Representative images of subcutaneous tumors of KPCY organoids treated with vehicle or FT206. (g) Immunohistochemical analysis of SLC2A1 staining in primary patient PDAC tumors. Scale bar is 50 μm. (h) Correlation between protein expression of SLC2A1 (% positive area) versus USP25 (% positive area) was assessed using linear regression. R-value and p-value are shown in graph inset. Source data are provided as a Source Date file.

Supplementary Figure 12. Graphical summary.

USP25 is highly expressed and active in PDAC, compared to normal pancreatic tissue. USP25 antagonizes polyubiquitination of HIF-1α, leading to HIF-1α stabilization and transcriptional activity. Enhanced HIF-1α transcriptional activity promotes metabolic reprogramming and tumor cell survival in the hypoxic tumor microenvironment.

Supplementary Table 1. Patient-derived organoids used in this study with detailed description of morphology, mutational status and primary tumour stage and histology.

PDO Line	PDO morphology	KRAS status	TP53 status	TNM Stage	Histology	Neoadjuvant Chemo?
K3T	non-cystic	missense mutation	missense mutation	T2N1M0	Poorly differentiated	None
K4T	cystic	missense mutation	missense mutation	T2N2M0	Moderately differentiated	None
K5T	non-cystic	missense mutation	no mutation	T3N2M0	Moderately differentiated	None
K7T	cystic	missense mutation	deep deletion	T4N1M0	Moderately differentiated	FOLFIRINOX 12 Cycles
K10T	non-cystic	missense mutation	missense mutation	T2N1M0	Moderately differentiated	None
K13T	cystic	missense mutation	no mutation	T2N1M0	Moderately differentiated	None
K17T	cystic	missense mutation	no mutation	Unknown	Moderately differentiated	None
K19T	cystic	missense mutation	nonsense mutation	Unknown	Moderately differentiated	None
K22T	non-cystic	missense mutation	missense mutation	T2N1M0	Moderately differentiated	None
K25T	non-cystic	missense mutation	missense mutation	T2N1M0	Moderately differentiated	None
K28T	cystic	missense mutation	missense mutation	T2N1M0	No diff. status	None
K36T	non-cystic	n/a	n/a	T3N1M0	Adenosquamous	None
K38T	cystic	missense mutation	n/a	T2N1M0	No diff. status	None
K46T	non-cystic	missense mutation	n/a	T2N2M0	Moderately differentiated	None

Supplementary Table 2. shRNA target sequences.

Gene name	Species	Clone ID	Sequence (5'-3')
YFP-1	N/A	N/A	ccgggaacggcatcaaggtgaacttctcgagaagttcacc ttgatgccgttcttttg
YFP-2	N/A	N/A	ccggcaacagccacaacgtctatatctcgagatatagacg ttgtggctgttgttttg
YFP-3	N/A	N/A	ccggggagcgcaccatcttcttcaactcgagttgaagaag atggtgcgctccttttg
Non-Target-1	N/A	SHC002	ccggcaacaagatgaagagcaccaactcgagttggtgct cttcatcttgttgttttg
Non-Target-2	N/A	SHC0016	ccgggcgcgatagcgctaataatttctcgagaaattattagc gctatcgcgcttttg
Usp8-1	Mu	TRCN0000030744	ccggcctcacatctaatgcttacaactcgagttgtaagcatt agatgtgaggttttg
Usp8-2	Mu	TRCN0000030745	ccggcgcagtttacaaccaatgctactcgagtagcattggtt gtaaactgcgttttg
Usp8-3	Mu	TRCN0000030746	ccggccaaaggattaacggcgagaactcgagttctcgcc gttaatcctttggttttg
Usp14-1	Mu	TRCN0000030758	ccgggagaagtttgaaggtgtagaactcgagttctacacctt caaacttctcttttg
Usp14-2	Mu	TRCN0000030757	ccgggcagctcttagagatttgtttctcgagaaacaaatctct aagagctgcttttg
Usp14-3	Mu	TRCN0000312005	ccgggagaagtttgaaggtgtagaactcgagttctacacctt caaacttctcttttg
Uchl3-1	Mu	TRCN0000030714	ccggtcttgacagaaacaccaaatactcgagtatttggtgttt ctgtcaagatttttg
Uchl3-2	Mu	TRCN0000030715	ccggcctgaacttcttagcatggtactcgagtaccatgctaa gaagttcaggttttg
Uchl3-3	Mu	TRCN0000030718	ccgggcatggtaccaagaccagtatctcgagatactggtct tggtaccatgctttttg
Usp19-1	Mu	TRCN0000030782	ccggcgatcctttgaagctgagattctcgagaatctcagctt caaaggatcgttttg
Usp19-2	Mu	TRCN0000030780	ccggcggcacaagatgagaaatgatctcgagatcatttctc atcttgtgccgttttg
Usp19-3	Mu	TRCN0000335553	ccggcggcacaagatgagaaatgatctcgagatcatttctc atcttgtgccgttttg
Usp48-1	Mu	TRCN0000086675	ccggccgaattgcttggttggcattctcgagaatgccaacc aagcaattcggttttg
Usp48-2	Mu	TRCN0000086673	ccgggctgtcaacaatttgctgaaactcgagtttcagcaaat tgttgacagcttttg
Usp48-3	Mu	TRCN0000086677	ccggctgaaggaagaacgattagaactcgagttctaatcgt tcttccttcagttttg
Usp7-1	Mu	TRCN0000087152	ccgggccgaatttaacagagagaatctcgagattctctctgt taaattcggcttttg
Usp7-2	Mu	TRCN0000087150	ccggcctgcaatgttagataatgaactcgagttcattatctaa cattgcaggttttg
Usp7-3	Mu	TRCN0000087151	ccgggcaacttatgaggttcatgtactcgagtacatgaacct cataagttgcttttg
Otud6b-1	Mu	TRCN0000113316	ccgggccagagaattggaaattaaactcgagtttaatttcca attctctggcttttg
Otud6b-2	Mu	TRCN0000113318	ccggccagacatcttgagagtgaaactcgagtttcactctc aagatgtctggttttg
Otud6b-3	Mu	TRCN0000113319	ccgggctgagtacatgcaaacccatctcgagatgggtttgc atgtactcagcttttg
Usp28-1	Mu	TRCN0000030868	ccgggctgttattcagtctctctttctcgagaaagagagactg aataacagcttttg

Usp28-2	Mu	TRCN0000030865	ccggcggaagttgaaggaggaaatactcgagtatttcctcc ttcaacttccgttttg
Usp28-3	Mu	TRCN0000030866	ccgggcagtacattcaggaagataactcgagttatcttcctg aatgtactgcttttg
Usp15-1	Mu	TRCN0000231399	ccggtgagaggtgaaatagctaaatctcgagatttagctatt tcacctctcatttttg
Usp15-2	Mu	TRCN0000231397	ccggcagactgtggaacaagtatatctcgagatatacttgtt ccacagtctgttttg
Usp15-3	Mu	TRCN0000033215	ccgggctgacacaatagatacgattctcgagaatcgtatct attgtgtcagcttttg
Uchl5-1	Mu	TRCN0000030724	ccgggcaatcaagatgactggattactcgagtaatccagtc atcttgattgcttttg
Uchl5-2	Mu	TRCN0000030726	ccgggtacgcatcaagatgtgcattctcgagaatgcacatc ttgatgcgtacttttg
Uchl5-3	Mu	TRCN0000030725	ccggcttgcctttcattatggaattctcgagaattccataatga aaggcaagttttg
Otud7b-1	Mu	TRCN0000311256	ccggggtagatattagggttgaatactcgagtattcaaccct aatatctacctttttg
Otud7b-2	Mu	TRCN0000308627	ccgggcagaaggaatggaatgaattctcgagaattcattcc attccttctgcttttg
Otud7b-3	Mu	TRCN0000308626	ccggcctttagtggagggagtacttctcgagaagtactccct ccactaaaggttttg
Otub1-1	Mu	TRCN0000030982	ccgggagcaagttcttcgagcacttctcgagaagtgctcga agaacttgctcttttg
Otub1-2	Mu	TRCN0000030983	ccgggtccatccaagtggagtacatctcgagatgtactcca cttggatggacttttg
Otub1-3	Mu	TRCN0000335250	ccgggagcaagttcttcgagcacttctcgagaagtgctcga agaacttgctcttttg
Usp5-1	Mu	TRCN0000030738	ccggcgaggatgtgaagattgtcatctcgagatgacaatctt cacatcctcgttttg
Usp5-2	Mu	TRCN0000030737	ccggcctgggctacatctacttctactcgagtagaagtagat gtagcccaggttttg
Usp5-3	Mu	TRCN0000030736	ccggcgaatgttcaaggccctcattctcgagaatgagggc cttgaacattcgttttg
Usp24-1	Mu	TRCN0000040628	ccgggctggattctttaggcagaaactcgagtttctgcctaa agaatccagcttttg
Usp24-2	Mu	TRCN0000086746	ccggcccgagctcttgtctgccattctcgagaatggcagac aagagctcgggttttg
Usp24-3	Mu	TRCN0000086745	ccggtcattggtctatcccgtacaactcgagttgtacgggat agaccaatgatttttg
Usp9x-1	Mu	TRCN0000030759	ccggcggcttaactttcttaggtttctcgagaaacctaagaa agttaagccgttttg
Usp9x-2	Mu	TRCN0000030763	ccggcctcaacaagtttggcactttctcgagaaagtgccaa acttgttgaggttttg
Usp9x-2	Mu	TRCN0000030761	ccgggcagaagaaatcactatgattctcgagaatcatagtg atttcttctgcttttg
Atxn3-1	Mu	TRCN0000123962	ccgggctcagaattgatcctataaactcgagtttataggatc aattctgagcttttg
Atxn3-2	Mu	TRCN0000123963	ccggctcgcactattcttggctcaactcgagttgagccaaga atagtgcgagttttg
Atxn3-3	Mu	TRCN0000123961	ccgggctcactttgtgctcagcattctcgagaatgctgagca caaagtgagcttttg
Otud4-1	Mu	TRCN0000252253	ccggccgtgtcacaagcgcatttaactcgagttaaatgcgc ttgtgacacggttttg
Otud4-2	Mu	TRCN0000252254	ccgggcgtttatagaagggtcatttctcgagaaatgacccctt ctataaacgcttttg
Otud4-3	Mu	TRCN0000252251	ccggcacgttagattggatcataatctcgagattatgatcca atctaacgtgttttg

Usp25-1	Mu	TRCN0000030827	ccggcccaacgatcactgcaagaaactcgagtttcttgcagtgatcgttgggtttttg
Usp25-2	Mu	TRCN0000233427	ccggttatatctggacaggtatatgctcgagcatatacctgtccagatataatttttg
Usp25-3	Mu	TRCN0000233428	ccggcatcgctggaggacggaaatactcgagtatttccgtcctccagcgatgtttttg
Usp25-4	Mu	TRCN0000233431	ccggtagtataatggaaccatattgctcgagcaatatggttccattatactatttttg
USP25-1	Hu	TRCN0000004366	ccgggcacttctcctgttgacgatactcgagtatcgtcaacaggagaagtgctttttt
USP25-2	Hu	TRCN0000004368	ccgggctgttcctcatctgtgcttactcgagtaagcacagatgaggaacagctttttt
USP25-3	Hu	TRCN0000004369	ccgggcgtgagctgaggtatctattctcgagaatagatacctcagctcacgctttttt
USP25-4	Hu	TRCN0000004370	ccggtggaggagtaagatgaaatatctcgagatatttcatcttactcctccatttttt
HIF1A-1	Hu	TRCN0000003808	ccggccgctggagacacaatcatatctcgagatatgattgtgtctccagcggttttt
HIF1A-2	Hu	TRCN0000003811	ccggcggcgaagtaaagaatctgaactcgagttcagattcttacttcgccgttttt
HIF1A-3	Hu	TRCN0000010819	ccggtgctctttgtggttggatctactcgagtagatccaaccacaaagagcatttttt

Supplementary Table 3. RT-qPCR primers.

Target	Species	FWD sequence (5'-3')	REV sequence (5'-3')
36b4	Mu/hu	gtgctgatgggcaagaac	aggtcctccttgtgaac
Tbp	Mu	cggtcgcgtcattttctc	gggttatcttcacacacca
Tbp	Hu	ccactcacagactctcacaac	ctgcggtacaatcccagaact
Atxn3	Mu	ggagacgagaagcctactttga	tggatatgaaaggggtccag
Otub1	Mu	gggtagcgactccgaagg	gattctgcacagcaatctcttg
Otud4	Mu	gatgccctcacagatcacaa	tggggagaggccaaaatagt
Otud6b	Mu	agaaggcatcggaaggaga	agcgttcttcattccctgaa
Otud7b	Mu	cggggttctgctcaaaag	tcatgggatcatcaggtactctc
Uchl3	Mu	agcagtcatggagggtcaa	agcagtcatggagggtcaa
Uchl5	Mu	gccaggagaagaacctgct	cctgagtggcacaagcatta
Usp5	Mu	ttcacctttggcttagactgg	gagctcctctggcatctcaa
Usp7	Mu	cccgaggacatggagatg	cattgatgacagggttctgagta
Usp8	Mu	caaaaagagacctgatttcaagc	tgatgtttgcaggtccaagt
Usp9x	Mu	tagtccgaggatctgccagt	aaaccgcacgttcttgct
Usp14	Mu	ggcgaacaagggcagtatc	tctgttgcaggactctcatca
Usp15	Mu	gctgtttccaaccactatggag	ccacttcccatcatctttgttt
Usp19	Mu	ggaaccggaatcgagagc	cttcagcaaagaaccaagagc
Usp24	Mu	cgagtctaccaaagataccttcact	gacgctgcctatcgtctcat
Usp25	Mu	cagtcggtctgaagaatgtcg	aactccaaaagattgaataatgactg
Usp28	Mu	ctgcttccttcggatcgtt	cactggaggcagctttgtaa
Usp48	Mu	agactcgaaactctgtcaaccttt	gctgggccatatgagagcta
USP25	Hu	tcagagacttctgtgacaacagc	tcacttcttgatggctgctcta
HIF1A	Hu	ttttcaagcagtaggaattggaa	gtgatgtagtagctgcatgatcg
HIF1B	Hu	ctgtcatcctgaagaccagcag	ctggttctcatccagagccattc
HIF2	Hu	ctgtgtctgagaagagtaacttcc	ttgccataggctgaggactcct
MYC	Hu	tctccttgcagctgcttag	gtcgtagtcgaggtcatag
ENO1	Hu	tcccaacatcctggagaataa	atgccgatgaccaccttatc
ENO3	Hu	ttgagaagaaggcctgcaa	cccccagccattagactg
HK1	Hu	tgaggttggactcattgttgg	ccaccatctccacgttcttc
LDHA	Hu	cgtcagcaagagggagaaag	gccacgtaggtcaagatatcc
PFKL	Hu	acacccgtgtaactgtgctg	atgcccatcttgctgctc
PKM	Hu	cagccaaaggggactatcct	caaataattgcaagtggtagatgg
SERPINE1	Hu	aaggcacctctgagaacttca	cccaggactaggcaggtg
SLC2A1	Hu	ggttgtgccatactcatgacc	gagataggacatccagggtagc
Hif1a	Mu	catgatggctccctttttca	gtcacctggttgctgcaata
Eno1	Mu	gaggcgcttagtgctgct	atagacatggcgaatttctgg
Eno3	Mu	gaggggtgaactgacactg	gagtcttctccacccgaaga
Hk1	Mu	gtggacgggacgctctac	ttcactgtttggtgcatgatt
Ldha	Mu	gctccccagaacaagattacag	tcgcccttgagtttgtcttc
Pfkl	Mu	attgaccggcatggaaag	aagcccagcctctgaacc
Pfkp	Mu	gagggaccccatctgcat	gtagcttccagcaaggcaat
Pkm	Mu	gcagcagctttgatagttctcag	tcgagtcacggcaatgatag
Serpine1	Mu	aggatcgaggtaaacgagagc	gcgggctgagatgacaaa
Slc2a1	Mu	gaccctgcacctcattgg	gatgctcagataggacatccaag

Supplementary Table 4. Electroporation settings for induction of PDO lines using the NEPA21 super electroporator from Nepagene.

Parameter	Poring Pulse	Transfer Pulse
Voltage	175V	20V
Pulse Length	5.0ms	50ms
Pulse Interval	50.0ms	50ms
Number of Pulses	2	5
Decay Rate	10%	40%
Polarity	+	+/-

Supplementary Table 5. Antibodies used for immunohistochemistry, immunofluorescence, and western blotting.

ANTIBODY	Company, product #	Dilution	Application
Rabbity anti USP25	Sigma-Aldrich; HPA024142	1:100x	IHC
Rabbit anti SLC2A1 (Glut1)	Alpha Diagnostics, GT11-A	1:100x	IHC
Rabbity anti Caspase 3	R&D Bio-Techne, AF825	1:100x	IHC
Rat anti CK19	Developmental Studies Hybridoma Bank, TROMA-III	1:100x	IHC
Goat anti GFP	Abcam, ab6673	1:100	IHC
Rabbit anti SLC2A1 (Glut1)	Alpha Diagnostics, GT11-A	1:100x	IF
Rat anti CK19	Developmental Studies Hybridoma Bank, TROMA-III	1:100x	IF
Mouse anti αSMA	Sigma-Aldrich, A5228	1:100x	IF
Donkey anti rat IgG Alexa Fluor488	Life Technology, A21208	1:200x	IF
Donkey anti mouse IgG Alexa Fluor546	Life Technology, A10036	1:200x	IF
Donkey anti rabbit IgG Alexa Fluor647	Life Technology, A31573	1:200x	IF
Mouse anti β-ACTIN	Abcam, ab49900	1:10000x	WB
Rabbit anti GAPDH	Abcam, ab9485	1:5000	WB
Goat anti GFP	Abcam, ab6673	1:2000	WB
Rabbit anti Histone 3B	Millipore, 06755	1:1000	WB
Rabbit anti HIF-1α	Novus, NB100-449	1:1000x	WB
Mouse anti FLAG-HRP M2	Sigma-Aldrich, A8592	1:10000	WB
Rabbit anti HIF-2	Cell Signaling, 7096	1:1000	WB
Rabbit anti ARNT (HIF-1β)	Cell Signaling, 5537	1:1000	WB
Rabbit anti HA	Sigma-Aldrich, H6908	1:1000	WB
Rabbit anti SLC2A1(GLUT1)	Alpha Diagnostics, GT11-A	1:1000	WB
Rabbit anti c-Myc	Abcam, Y69 clone, ab32072	1:1000	WB
Rabbit anti USP25	Abcam, ab187156	1:2000	WB
Rabbit anti USP28	Sigma, HP006779	1:1000	WB
Mouse anti V5 (tag)	Invitrogen, R960-25	1:5000	WB
Rabbit anti VHL	Cell Signaling, 68547	1:1000	WB

Supplementary Figure 1

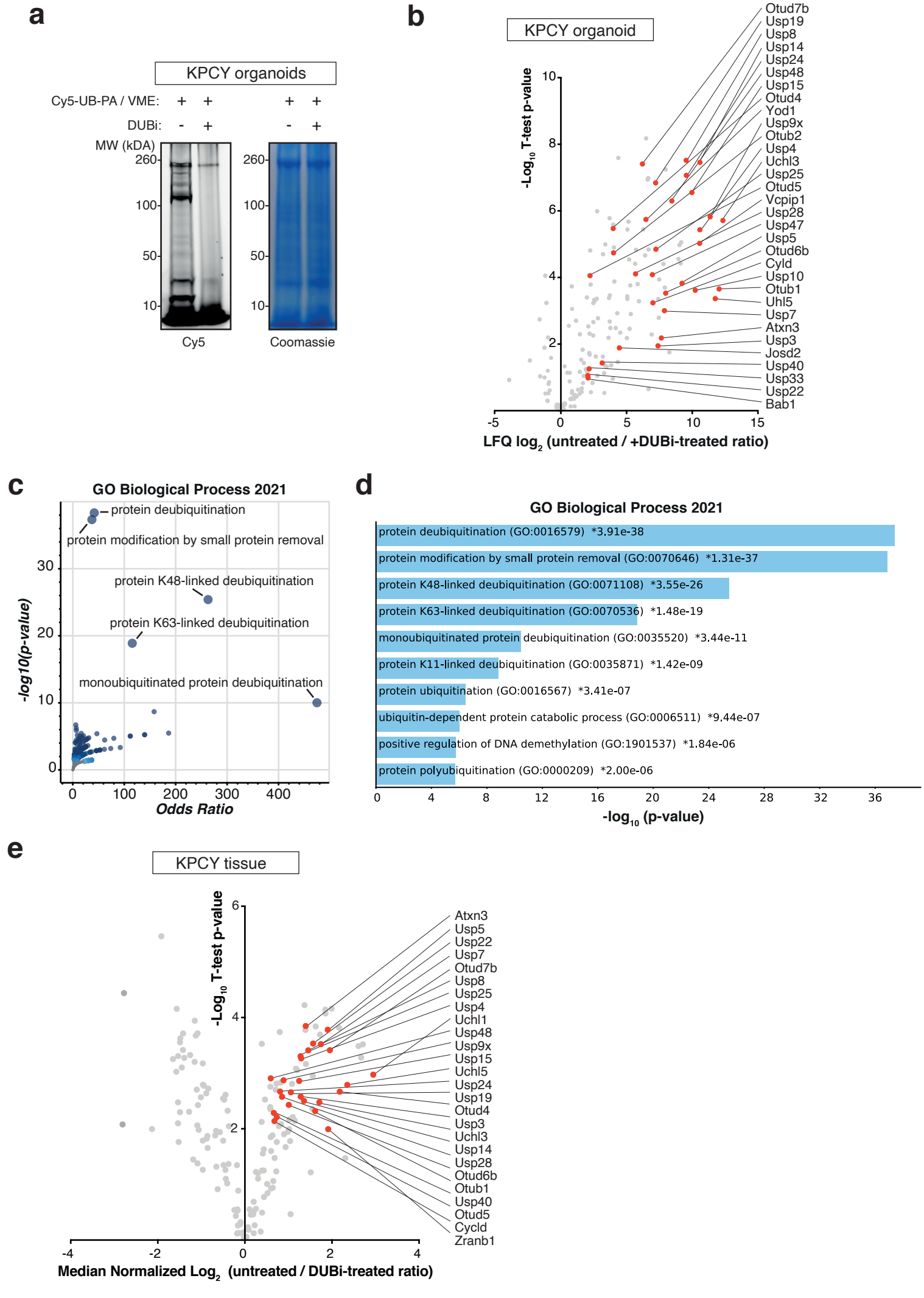

Supplementary Figure 2

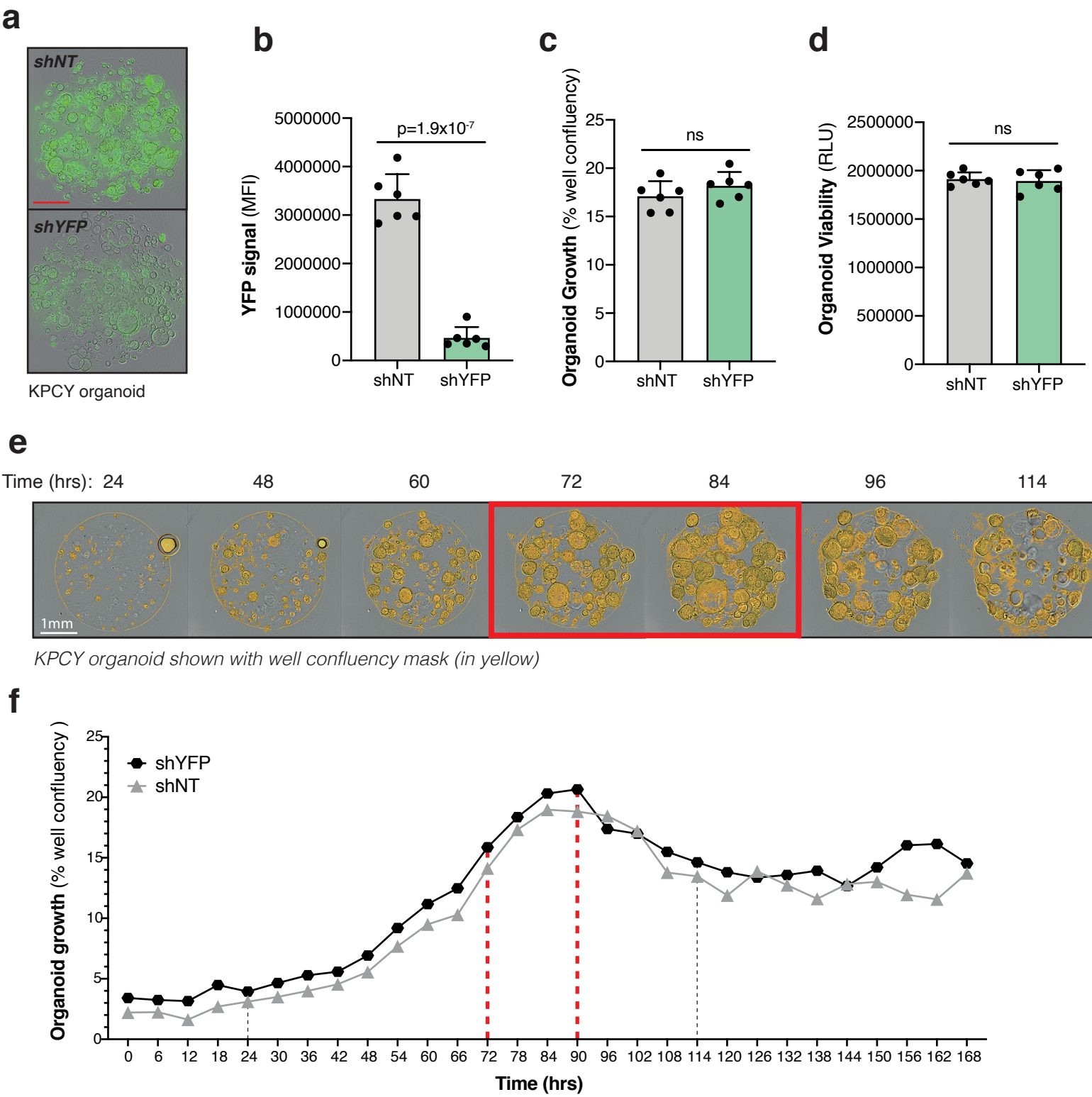

Supplementary Figure 3

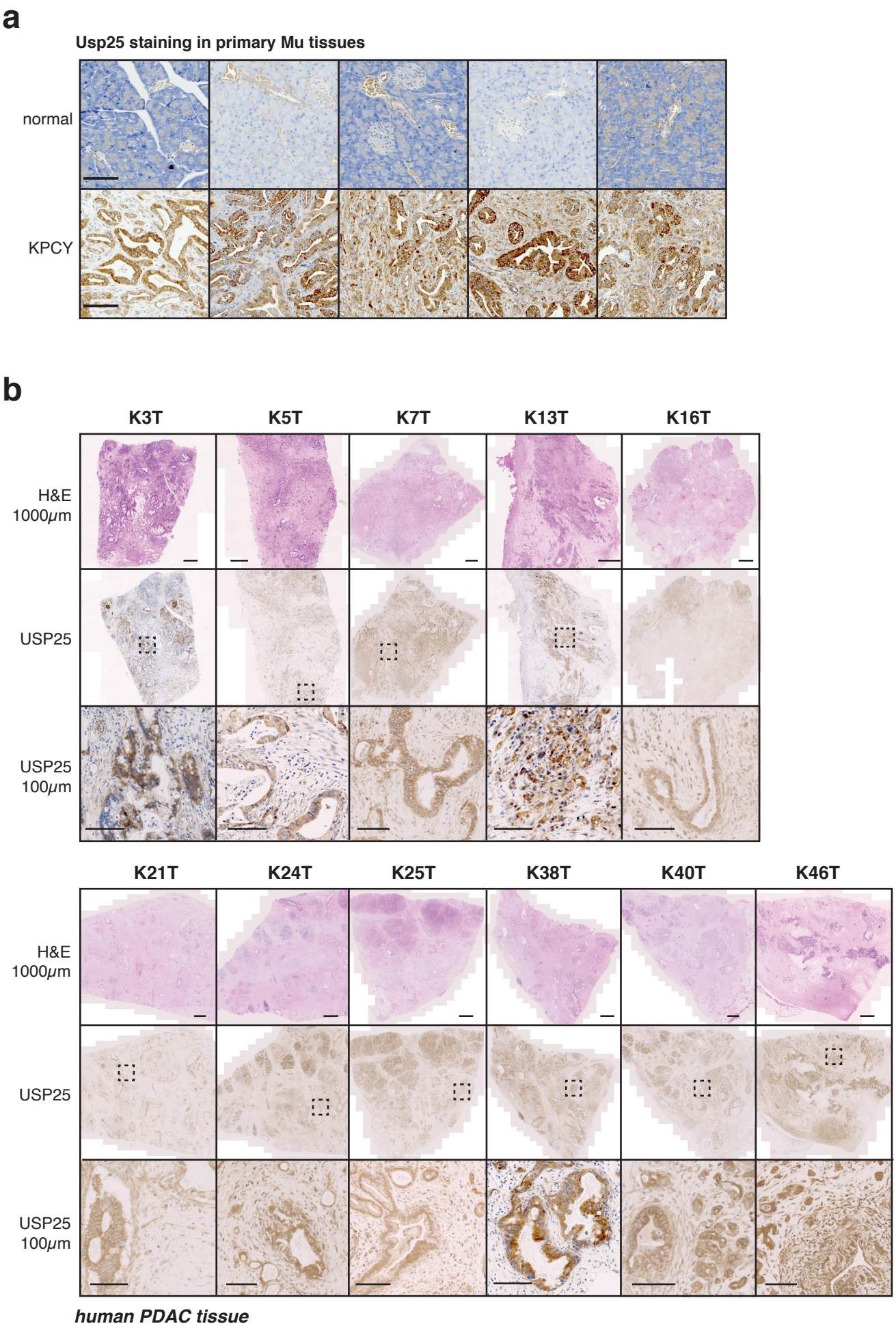

Supplementary Figure 4

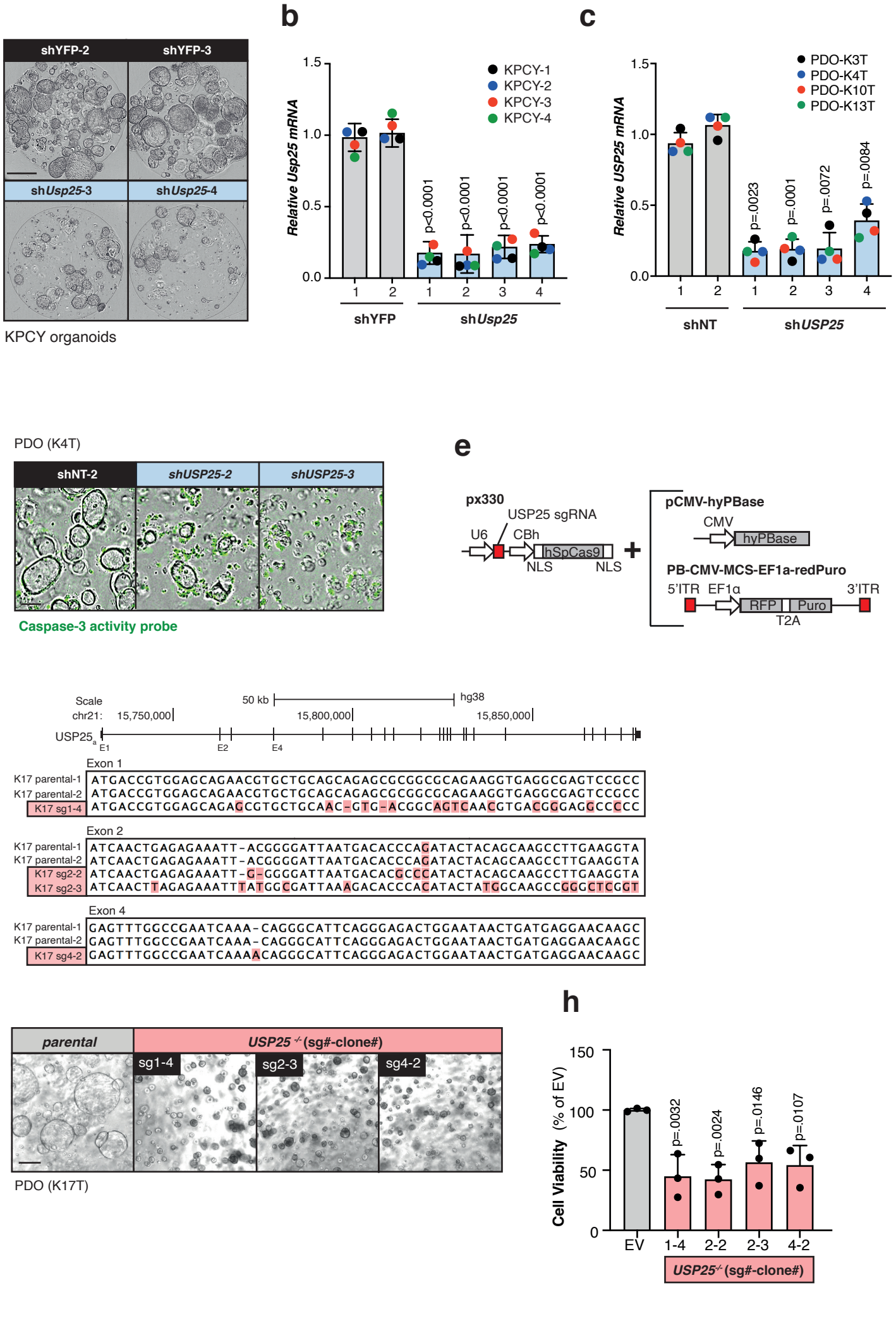

Supplementary Figure 5

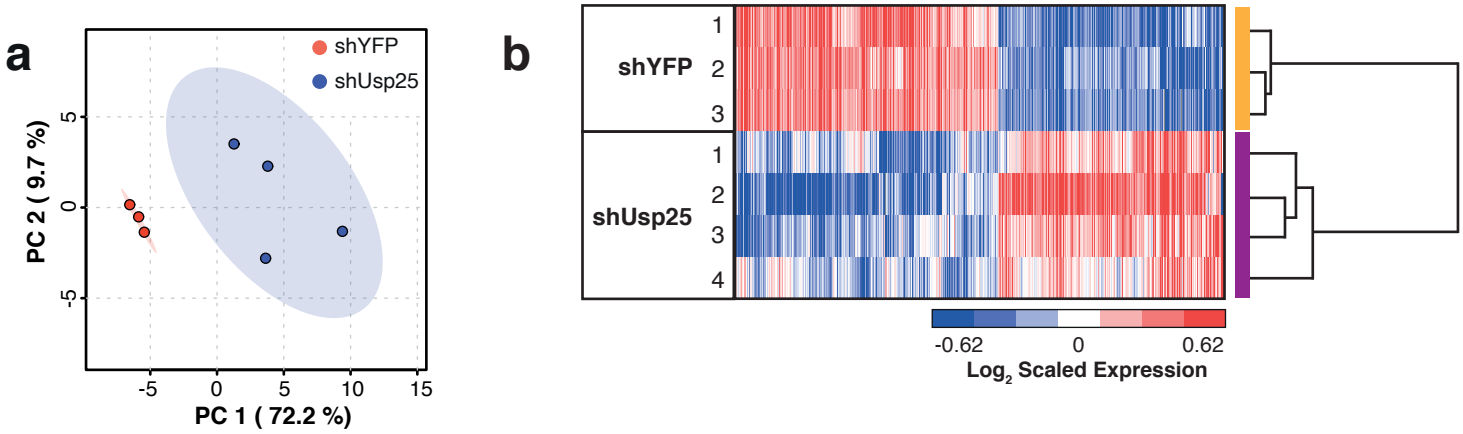

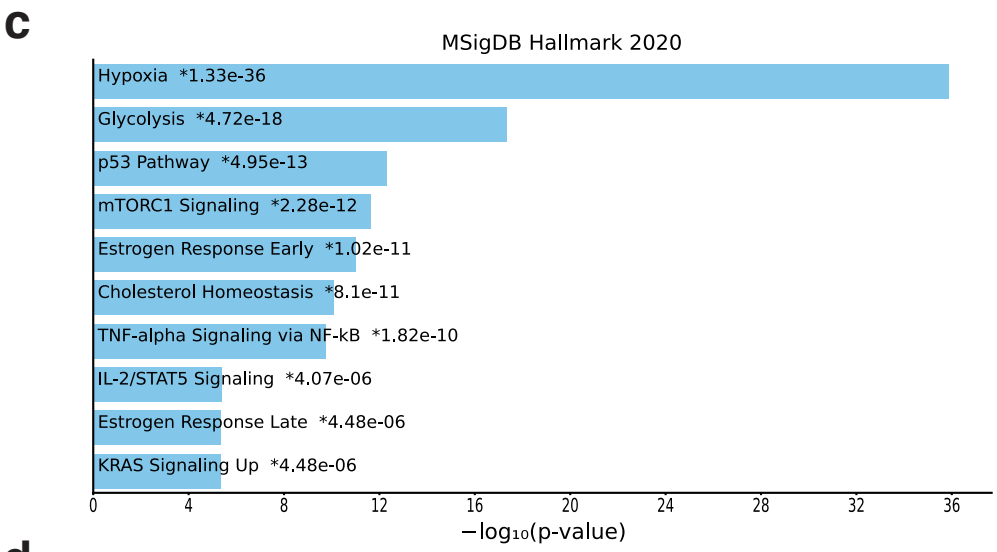

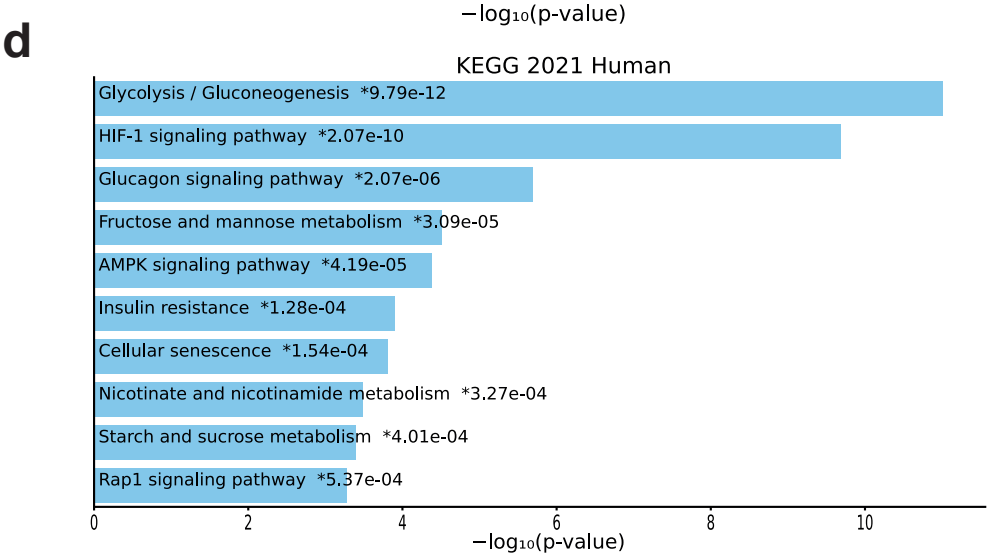

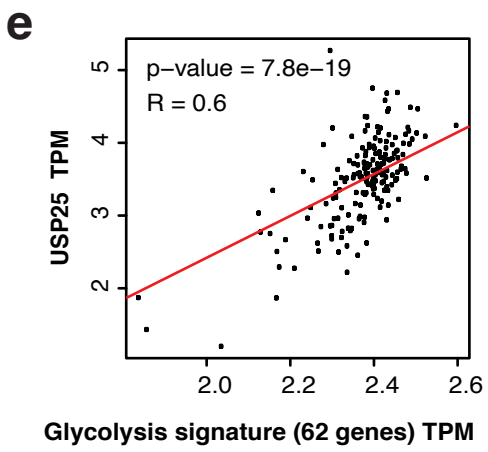

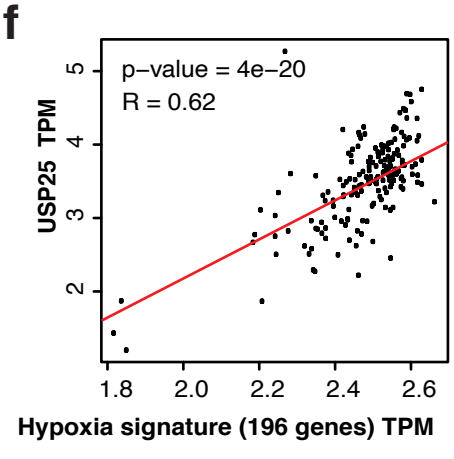

Supplementary Figure 6

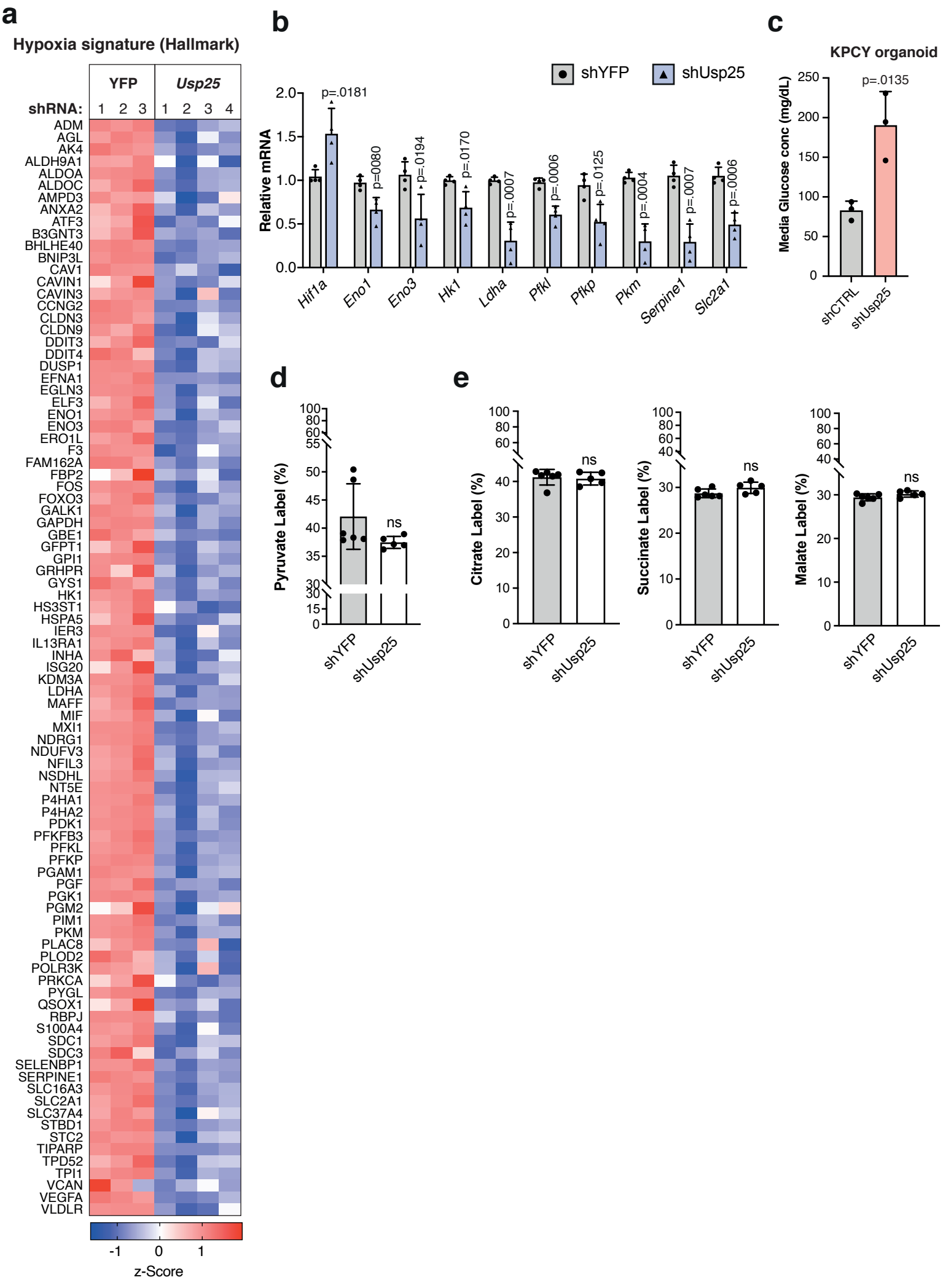

Supplementary Figure 7

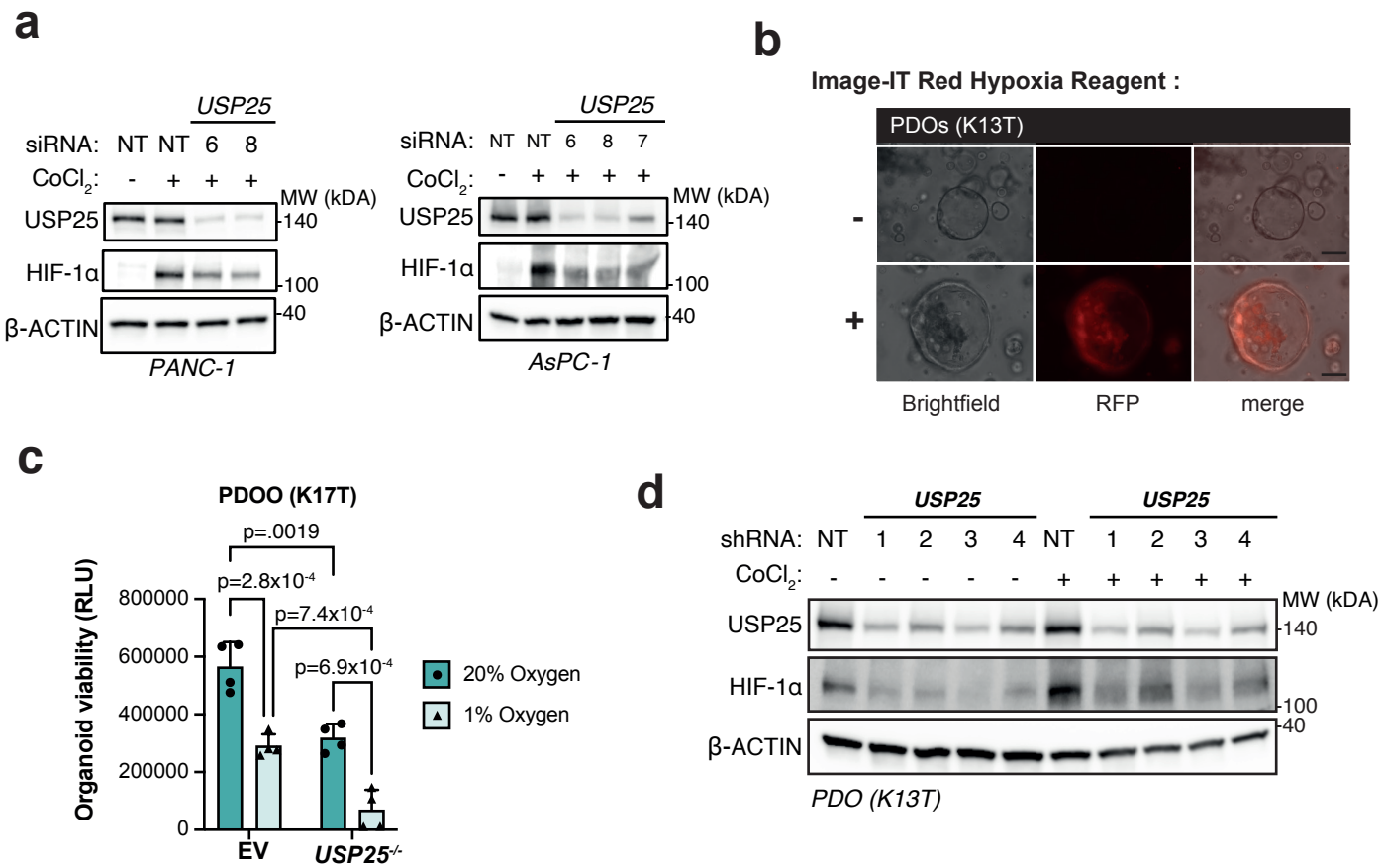

Supplementary Figure 8

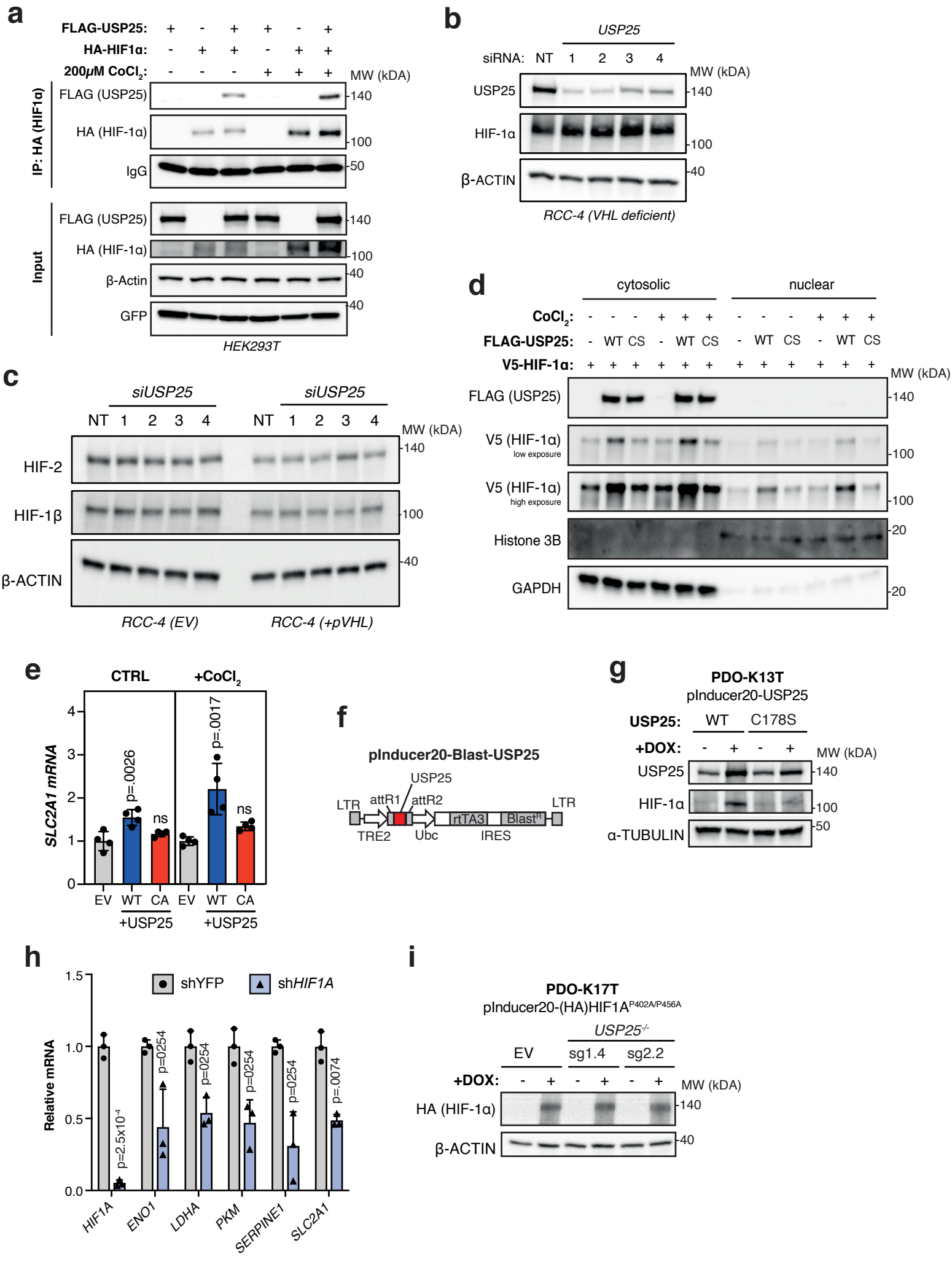

Supplementary Figure 9

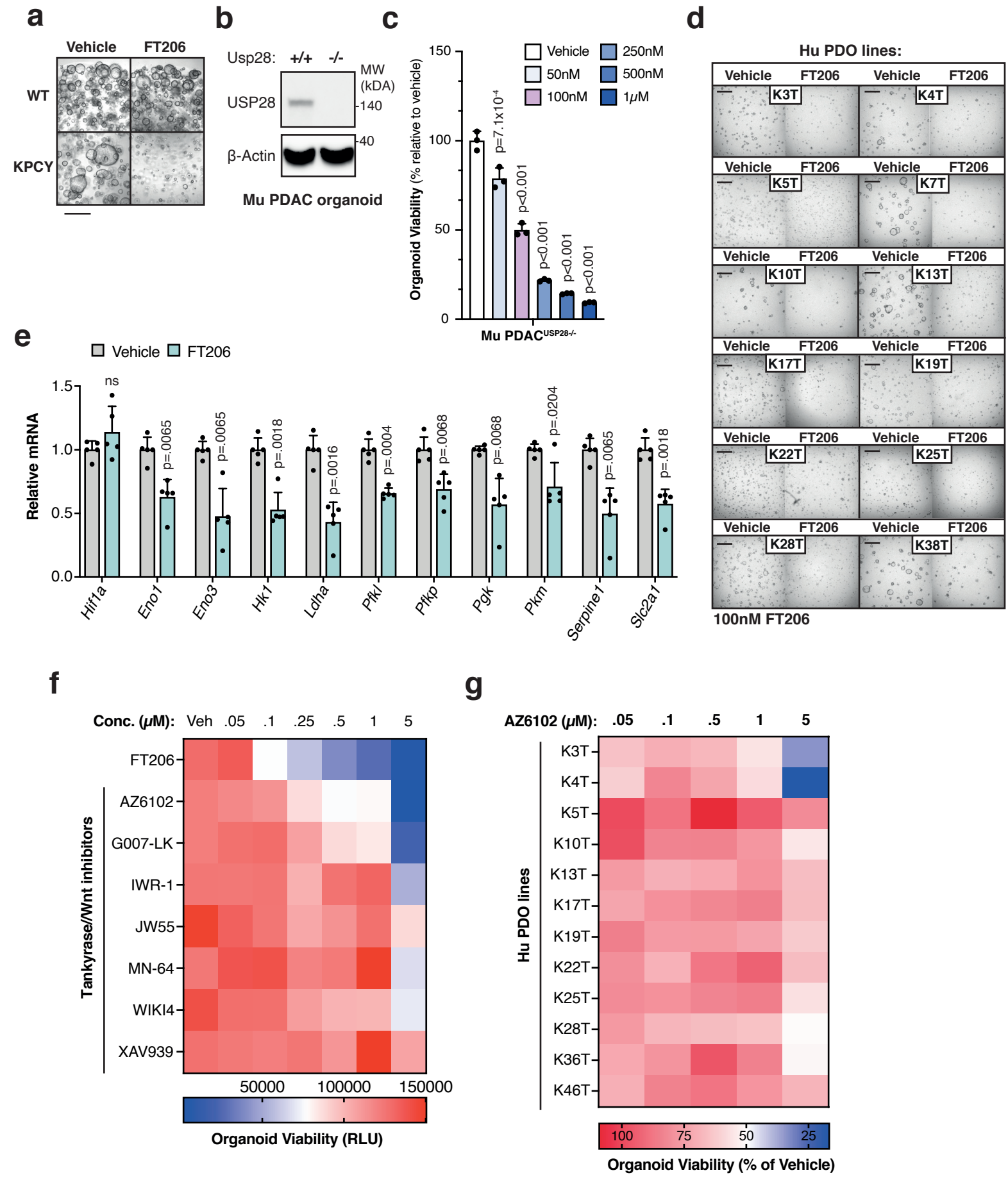

Supplementary Figure 10

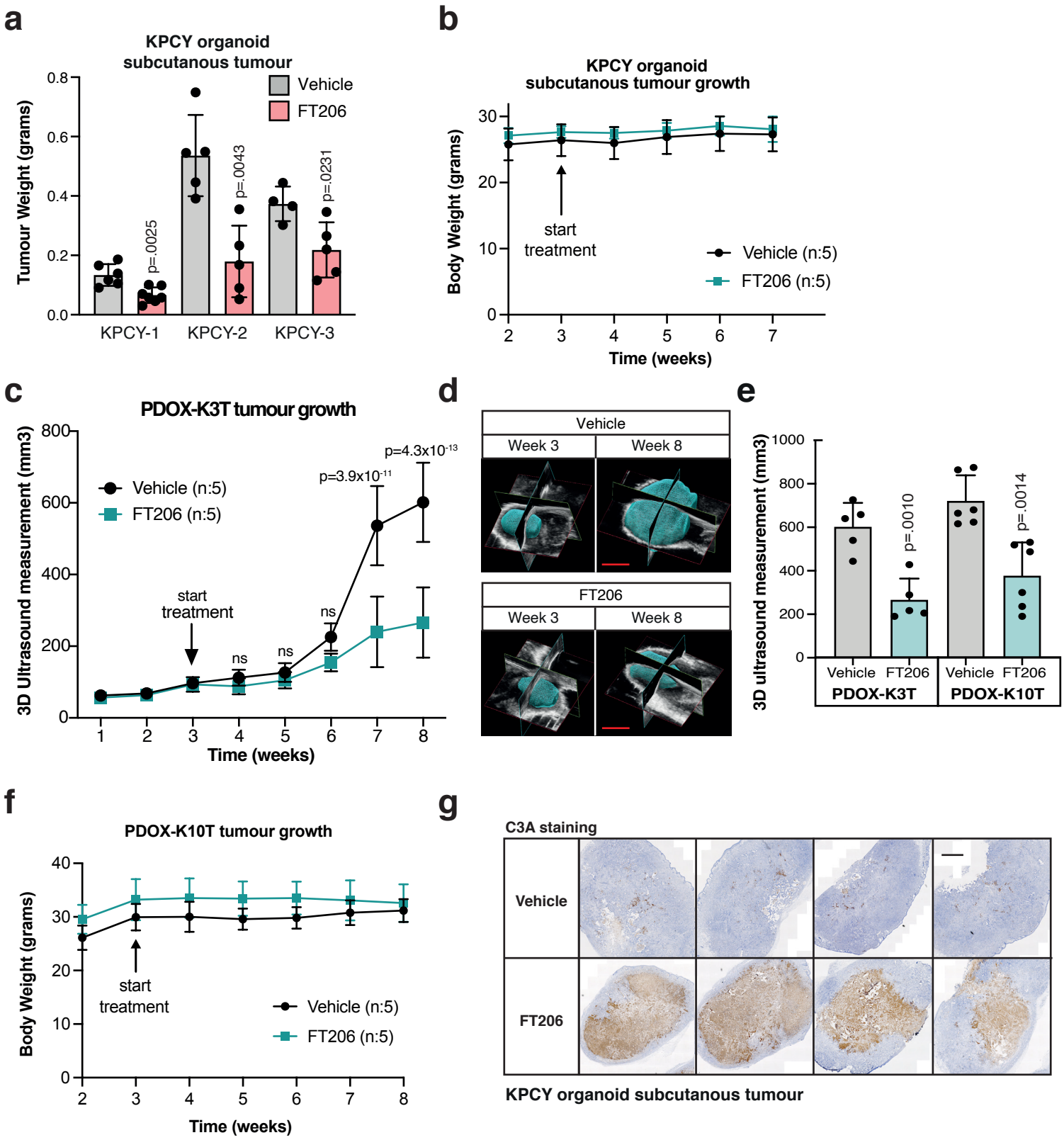

Supplementary Figure 11

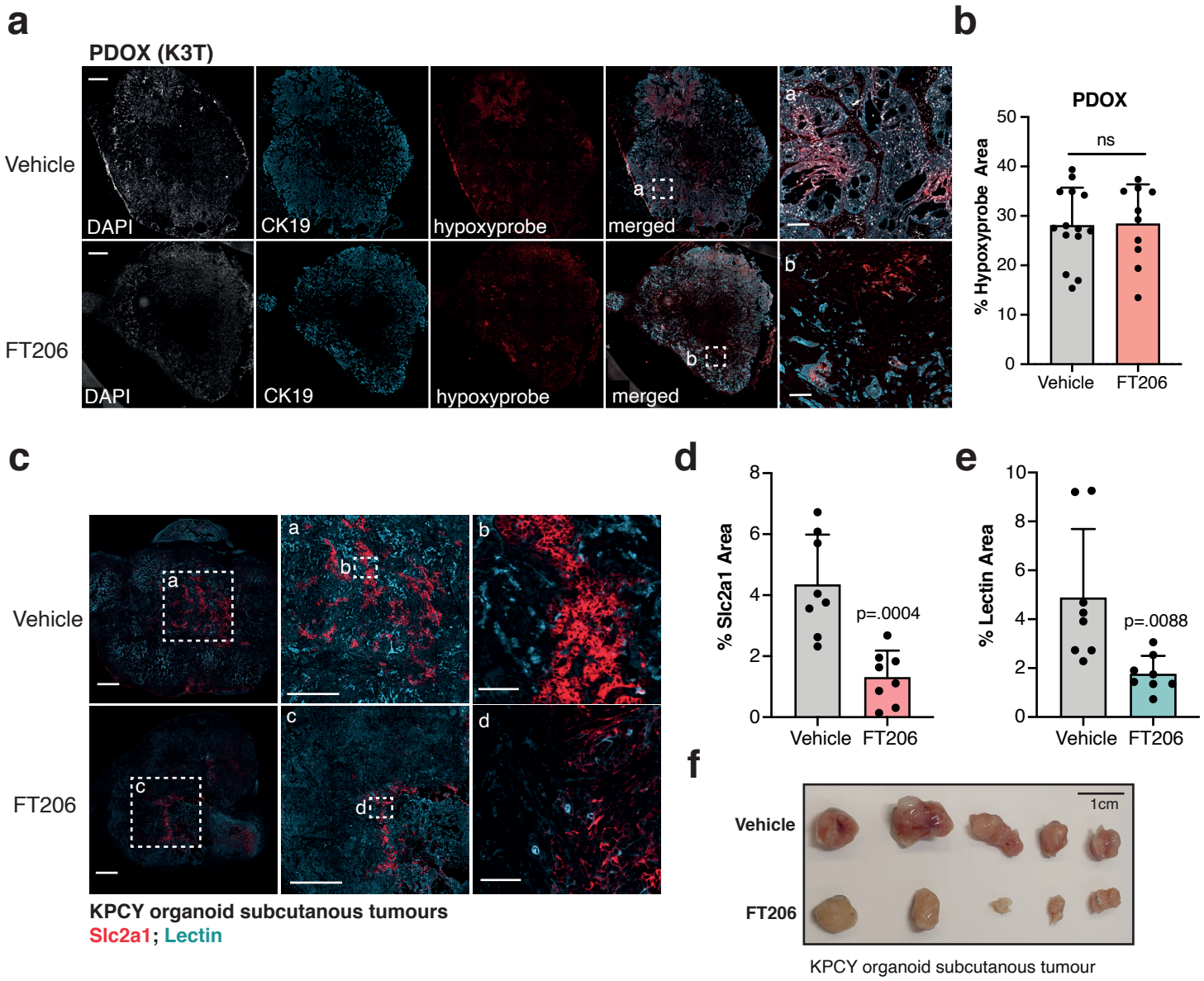

Supplementary Figure 12